

MWC 603, A HIGH-VELOCITY SYMBIOTIC STAR

WILLIAM G. TIFFT* AND JESSE L. GREENSTEIN

Mount Wilson and Palomar Observatories
 Carnegie Institution of Washington, California Institute of Technology
 Received September 3, 1957

ABSTRACT

The star MWC 603 is a faint symbiotic star, M3ep + O, at relatively high galactic latitude, and possibly a member of population II. Its light is slightly variable, at least in the ultraviolet. The absorption lines of the M3 star have essentially the same velocity as the emission lines, both permitted and forbidden. The excitation is not so high as in AX Per, but lines of He II, C III, N III, O III and [O III], [Ne III], [Fe V], and possibly [Fe VI] and [Ne IV] are present. The stability of this star contrasts with the large velocity and light-variations found in most symbiotic objects. There is a good correlation between the diffuseness of emission lines and level of excitation.

Star No. 603 in the Mount Wilson catalogue of emission line objects was selected for observation because of the possibility that it might be a relatively high-latitude Be star. Spectra obtained by Greenstein at the coudé focus of the Hale reflector showed that the star was a high-velocity, peculiar object similar to the symbiotic stars. At the present time, eight spectra, dispersions 18, 27, and 38 Å/mm, have been obtained, and the star has been observed photoelectrically with the 60-inch telescope at Mount Wilson.

Previous studies of the star are limited to the reference in the emission-star catalogue (Merrill and Burwell 1943) and an unpublished proper motion by Vyssotsky, who discovered this object. Vyssotsky has very kindly permitted us to quote the proper motion, together with estimated probable errors. Vyssotsky finds $\mu_\alpha = +0''.006 \pm 0''.005$, $\mu_\delta = +0''.007 \pm 0''.005$ reduced to absolute motions. MWC 603 is located at $18^{\text{h}}20^{\text{m}}05^{\text{s}}$, $+23^\circ25'.5$ (1950), which corresponds to galactic co-ordinates $l = 19^\circ$, $b = +15^\circ$. (Please note that the declination of this star is here given correctly; there has been confusion in the published values.)

The spectrum appears composite, and the photoelectric measures taken on the U , B , V system amply confirm the apparent duplicity. The spectrum is characterized by great numbers of emission lines, and increasingly longward by an underlying absorption spectrum. Merrill has classified the absorption spectrum as about M3. On the best-exposed plates TiO bands are well marked. The emission lines indicate excitation by a very high-temperature source such as an O or W star. The emission-line spectrum is dominated by H, He I, He II, and Fe II. The C, N, O group is doubly ionized, and lines of the singly ionized atoms of the group are only weakly visible. Silicon is probably present in several stages of ionization. Forbidden lines of [O III], [Ne III], [Fe V], possibly [Fe VI] and a few other ions are present. The emission lines differ markedly in sharpness or fuzziness. Figure 1 shows sections of the spectrum as it appeared in August, 1954 and 1956.

PHOTOMETRY

Photoelectric observations are given in Table 1 as obtained at the 60-inch telescope on Mount Wilson and referred to the U , B , V system. The photometer and filters have been described elsewhere (Walker 1954). All observations have been referred to a comparison star $40''$ due north of MWC 603, and this star was tied into the fundamental Johnson system on four nights, two of which were quite good. Both M67 and IC 4665 have been used as reference standards. The comparison star appears to be non-variable with mean photometric data given in the last line of Table 1; its colors correspond closely to K5 V. The probable errors of the tie-in are 0.01, 0.01, and 0.02 mag. for V , $B - V$, and $U - B$.

* National Science Foundation Predoctoral Fellow.

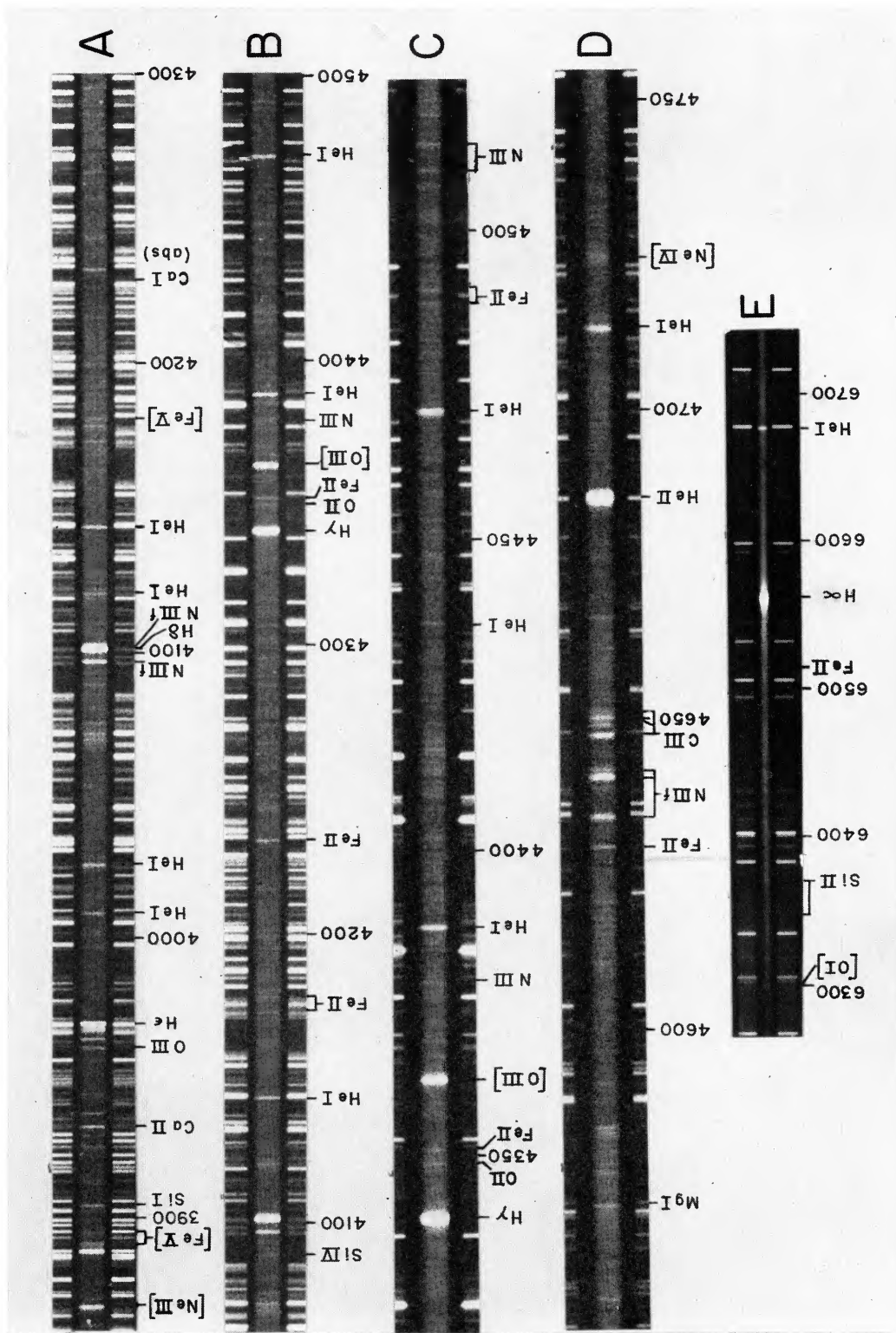


Fig. 1.—Palomar coude spectra (positives) of MWC 603. *A*, *B*: λ 3860–4495, original 38 Å/mm, August, 1954. Note breadth of [Fe V] compared to [Ne III], and the sharpness of Ca II and Si I. Lines possibly affected by the Bowen fluorescence mechanism are labeled N III, f. A shallow Ca I stellar absorption is marked at λ 4227. *C*, *D*: Original dispersion 18 Å/mm, August, 1956, copied to high contrast. Traces of absorption lines are seen, and the TiO bands contribute to the complex structure near λ 4600. Note change in the O II/Fe II ratio, shown by λ 4349/ λ 4352 on *C* as compared to *B*. Note the diffuse high-excitation (non-fluorescent) line of N III at λ 4379, and the diffuse feature at λ 4725, probably [Ne IV]. *E*: Red region, original 27 Å/mm, August, 1955 (Ne comparison). In view of the redness of the star, the strength of H α is obviously very great.

respectively. The probable errors of individual observations of MWC 603 are about 0.02, 0.01, and 0.04 mag. for V , $B - V$, and $U - B$, respectively.

It should be pointed out that, because of the large amount of light contributed by emission lines, the color-transformation equations used to convert instrumental magnitudes and colors to standard magnitudes and colors are probably not quite correct. Hence there may be significant systematic deviations from the U , B , V system defined by slightly different filter and photocell combinations. Because of the effect of emission lines, synthetic colors constructed by adding together an O and an M star serve only to indicate roughly the magnitude difference of the components. To a first approximation, the effect of emission lines in the V and U regions seems comparable, so the effect on the $U - V$ color is not serious. A fit to $U - V$ has been found by combining an M2 III and a B0 V star and assuming no reddening in MWC 603. Normal colors have been taken from the work of Johnson and Morgan (1953). Depending upon the particular date used to obtain a fit to the observed $U - V$ color of MWC 603, the red component is found to be from 1.4 to 2.2 mag. brighter than the blue component, in visual light. In the blue, the contributions are comparable, while in U the blue source dominates by about 3 mag.

TABLE 1
PHOTOELECTRIC OBSERVATIONS

Date	V	$B - V$	$U - B$	Date	V	$B - V$	$U - B$
1955 March 25	11 ^m 57	+1 ^m 04	-0 ^m 34	1956 May 10	11 ^m 45	+0 ^m 95	-0 ^m 66
March 26	11 54	+1 06	-0 30	May 11	11 43	+0 96	-0 67
March 28	11 55	+1 08	-0 33	May 13	11 42	+0 97	-0 65
March 28	11 54	+1 05	-0 27	June 14	11 56	+0 94	-0 78
1956 May 10	11 45	+0 95	-0 68	Comparison star	11 62	+1 16	+1 14

If we correct the MWC 603 observation for some reddening, the synthetic model will require a relatively stronger blue source. Further indication of the relative brightness of the red and blue sources is obtainable from the spectra. In an M-type spectrum the central intensity of λ 4227 of Ca I is essentially zero; in the composite, all the light in the center of the line can be ascribed to the blue source. Because of the complications arising from weak emission and absorption features, the estimate is fairly rough; in August, 1956, the depth of λ 4227 was close to 50 per cent, suggesting that the blue and red sources were about equally bright in B at this wave length. There is reason to think that the blue source was then relatively weak, since a comparable plate obtained in July, 1955, showed a much stronger ultraviolet continuum. It seems probable that the red source is usually at least 2 mag. brighter than the blue source in M_v .

The photometry shows that light and color changes are present. From the changes seen in the spectrum of the ultraviolet continuum, at least part of the change in the ultraviolet light is due to variation in the continuous radiation. In the yellow, the late-type spectrum dominates and appears fairly constant in brightness; the small changes shown by the photometry are possibly due either to a slight variation in emission-line strength or to the blue source. Changes in light or color do not appear to be rapid, since the two cases where several observations are available within a 4-day interval showed no significant variation. Without a considerably greater number of observations, nothing can be said about the regularity or irregularity of variations present.

VELOCITY MEASUREMENTS AND LUMINOSITY

Table 2 summarizes the radial-velocity measurements. All velocities refer to the emission lines, except the plate of July 12, 1955, on which several of the best absorption fea-

tures were measured. There appears to be no significant difference between the emission- and absorption-line velocities at this date. A somewhat poorer determination of the absorption-line velocity was made on the last plate and gave a velocity 5 km/sec more negative than the emission, but with a scatter of measures too large to give much significance. The absorption features are, at best, difficult to measure because of the distortion by weak emission features or blends in the complex absorption spectrum. There are no large velocity differences between emission lines of different elements or excitations. Table 3 shows the analysis of the velocities for the July, 1955, plate according to individual elements or closely related groups. Only the best-represented elements are included, except for the forbidden lines. There appears to be a slight tendency for velocity to cor-

TABLE 2
RADIAL-VELOCITY OBSERVATIONS

Date	Dispersion (Å/mm)	Velocity (km/sec)	p e (km/sec)	Remarks
1954 August 19	38	-68 3	±1 35	Emission lines Absorption lines Region near H α
August 22	38	-66 0	±0 89	
August 22	38	-65 6	±1 01	
November 7	18	-59 6	±0 79	
1955 July 12	18	-56 2	±0 46	
July 12	18	-56 8	±2 42	
August 6	27	-47 8	±1 04	
August 15	18	-62 8	±0 60	

TABLE 3
RADIAL VELOCITIES IN JULY, 1955

Identity	Velocity (km/sec)	p e (km/sec)	Identity	Velocity (km/sec)	p e (km/sec)
O II	-51 1	±1 4	He I	-56.8	±1 2
Fe II	-54 8	±0 8	H	-59 0	±1 3
C, N, O III	-56 7	±1 2	[O III], [Ne III]	-64 0	±2 1

relate with excitation, while the forbidden lines are almost certainly of somewhat higher negative velocity.

The over-all velocity appears to be at least slightly variable, although the largest differences are seen between plates of different dispersions or spectral regions; they could be the result of systematic effects. The over-all average velocity is close to -60 km/sec. Most of the symbiotic stars have variable but low radial velocity, in the mean, combined with large differences in the velocity given by absorption and emission lines, e.g., Z CMa, RY Sct, Z And. The latter may be explained as a P Cygni effect and is absent in MWC 603. Only RW Hya is at high latitude and has appreciable proper motion.

The distance and absolute magnitude of MWC 603 can be estimated by using the proper motion and radial velocity or by assuming models consistent with the observed characteristics of the star. MWC 603 lies only 7° from the solar apex; hence the solar motion adds directly to the radial velocity but affects the proper motion negligibly. The total proper-motion vector of MWC 603, though small, lies essentially parallel to the galactic equator but is of opposite direction from that expected from galactic rotation.

Including galactic rotation and solar motion, where significant, we can write the statistical relation between proper motion and radial velocity for this case as follows:

$$|4.74 r \mu - V_{t\theta}| = \sqrt{3} |V_r - V_{\odot} - V_{r\theta}|, \quad (1)$$

where μ is the total proper motion, V_r is the observed radial velocity, V_{\odot} is the solar motion, and $V_{t\theta}$ and $V_{r\theta}$ are the tangential and radial components of galactic rotation. We assume that the observed V_r refers to the star as a whole and does not represent motion in the envelope. Expressing $V_{t\theta}$ and $V_{r\theta}$ in terms of r by means of the first-order galactic-rotation relations and solving for r yields a distance $r = 2600$ parsecs. At this distance the simple galactic-rotation equations begin to break down. But if one uses directly the model of van de Hulst, Muller, and Oort (1954), the change is not very large, yielding a distance close to 2000 parsecs. If we assume an absorption of 0.5 mag., the luminosity found is $M_v = -0.5$. (Absorption cannot be very large because the region around MWC 603 contains some galaxies.) For the distance $r = 2000$ parsecs, the radial and tangential velocities, corrected for solar motion and galactic rotation, are -70 and $+120$ km/sec. The latter value, because of the small value of μ , is largely indeterminate.

The result $M_v = -0.5$ is consistent with a binary model consisting of a population I, M giant combined with a hot, subluminescent dwarf. An alternative model would be a red giant for which mass loss in the envelope has partially exposed part of the hot core. The rather high latitude and high velocity speak against population I membership; nevertheless, Greenstein, MacRae, and Fleischer (1956) have demonstrated that some objects apparently of population I are present at high latitudes. MWC 603 spectroscopically resembles such stars as CI Cygni and AX Persei, which lie at lower latitudes.

Because of the latitude and fairly high velocity of MWC 603, it is worthwhile to consider a population II model. The fact that the red component is several magnitudes brighter than the blue component, in visual light, suggests that we might construct a model with a population II, bright M giant, from the very top of the red giant branch of color-magnitude arrays for population II systems. (Normally these sequences stop at K II.) We might combine such a star with a hot, horizontal branch star or propose that mass loss in the envelope of the supergiant has partially uncovered the hot core. Such models would have M_v about -3 and, with a half-magnitude of absorption, would lie at a distance of 6500 parsecs. Using the galactic-rotation model of van de Hulst *et al.* (1954), we find that the radial and tangential velocities corrected for solar motion and galactic rotation are -85 and $+490$ km/sec, respectively. The very large tangential velocity seems implausible, but the uncertainty in the small proper motion makes the tangential velocity very uncertain; hence this model cannot be excluded. At a distance of 2000 parsecs, the star lies 500 parsecs above the galactic plane, so that a population I object of high initial luminosity leaving the plane with large z -velocity could undergo marked evolutionary changes before reaching the present location of MWC 603. If we accept a population II model, the star is unquestionably old and should show marked evolutionary effects. Another probable population II star of the symbiotic type is RW Hydrae, which is at even higher galactic latitude than MWC 603. Its proper motion of $0''.036$ yields a very large tangential velocity, although the radial velocity is low.

IDENTIFICATIONS AND SPECTRUM

Table 4 lists the identified emission features measured on two or more of the available plates. The last plate is not included, since only selected bright features were measured for velocity. The strongest, most certain, lines shortward of $\lambda 3860$ and longward of $\lambda 4925$ are included, although only a single plate covers these regions. The first column gives the mean of the measured wave lengths after each plate was corrected for the individual plate mean velocity. The second column gives the identification and multiplet

TABLE 4
EMISSION LINES PRESENT IN MWC 603

λ^*	IDENTIFICATION	INTENSITY		
		Pd 2166	Pd 2764	I'
(3662 6)	[Fe VI]	1 NN	0	
3665 96	H27	1 N		
3667 64	H26	1 N		
3669 49	H25	2 N		
3671 34	H24	2 N		
3673 82	H23	2 N		
3676 35	H22	2 N		
3679 27	H21	3 N		
3682 72	H20	3 N		
3686 82	H19	3 N		
3691 51	H18	3 N	2 N	
3697 05	H17	3 N	2 N	
3703 71	H16, O III—14, O III—21, C III—12	4 NN	2 NN	
3707 35	O III—14	2 N	1 N	
3711 94	H15	4 N	3 N	
3715 00	O III—14	3 N	2 N	
3721 86	H14	5 N	3 N	
3734 28	H13	5 n	3 n	
3750 14	H12	6 n	4 n	
3754 66	O III—2, N III—4, [Fe v]	5 N	4 N	
3757 26	O III—2	3 N	2 N	
3759 82	O III—2	6 N	5 N	
3770 60	H11	7 n	5 n	
3773 77	O III—2	2 NN	1 NN	
3783 43	Fe II—14	{1 NN
3784 66	He I—64 } [Fe v]	{1 NN
3791 17	O III—2	2 N
3797 79	H10	8	7	...
(3813 9)	[Fe VI]	1 NN	1 NN	
3819 70	He I—22, [Fe v]	3 N	2	
3833 50	He I—62	1 S	1 S	
3835 42	H9	9	8	
(3839 5)	[Fe v], [Fe v]	2 NN	2 NN	
3848 20	[Fe II], Mg II—5	2 S	2 S	
3856 02	Si II—1	2 S	2 S	
3862 61	Si II—1	3 s	3 s	
3868 78	[Ne III]	10 NN	9 NN	
3871 75	He I—60	2 s	2 s	
(3874 5)	[Fe II]	1	1	
3878 34	He I—59	2	1	
3889 00	H8, He I—2, C III—15	10	11	
(3891 6)	[Fe v], [Fe VI]	6 NN	6 NN	
(3895 6)	[Fe v]	4 NN	4 NN	
3895 99	Fe II—23	:
3905 53	Si I—3, [Fe II]	2 s	2 s	.
3914 47	Fe II—3	1 s	2 s	.
3926 50	He I—58	3	4	
3930 32	Fe II—3	1	1	
3933 52	Ca II—1	3 N	3 N	
3936 00	He I—57	1	1 S	
3938.26	Fe II—3, N III—8	3 SS	4 SS	
3945 14	Fe II—3, O II—6	1	2	
3961 61	O III—17	5 NN	5 NN	
3964 78	He I—5	5 s	6 s	
3966.18	Fe II—3	0
3967 38	[Ne III]	4 NN	5 NN

* A dagger following wave length indicates laboratory wave lengths; parentheses indicate interpolated on tracings. Multiplet numbers are from the *Revised Multiplet Table*.

TABLE 4—Continued

λ^*	IDENTIFICATION	INTENSITY		
		Pd 2166	Pd 2764	I'
3968 32	Ca II—1	4 NN	5 NN	
3970 08	He	12	14	
3973 14	O II—6			0
3974 10	Fe II—29			0
4009 28	He I—55	5 s	6 s	
4025 41	He II—3, He I—19			1
4026 33	He I—18	5 NN	8 NN	
4035 22	Fe II—22			0
4064 72	Fe II—39			0
4067.80	C III—16			0
4068 70	C III—16			2
4069 94	C III—16, O II—10	4 N	3 N	
4072 06	O II—10, [Fe V]	4	3	
4074 14	O III—23			1
4075 78	O II—10	5	3	
4078 90	O II—10			1
4080 94	O III—23			1
4081 80	Ca III—4			0
4089.07	Si IV—1	4 NN	4 NN	
4093 17	O II—10	1	2	
4094 28	O II—10			0
4097 30	N III—1	10 N	10 N	
4101 70	H δ	15	17	
4103 28	N III—1, Si I—2	6 N	7 N	
4104 78	O II—20			0
4106 26	O II—10			0
4110 38	Ca II—17, O II—37			0
4116 16	Si IV—1	1 N	2 N	
4119 32	O II—20, Fe II—21	2 N	2 N	
4120 86	He I—16, O II—19, O II—20	5 N	5 N	
4122 51	Fe II—28	2 N	2 N	
4124 76	Fe II—22			1
4128 63	Fe II—27	1 N	2 N	
4132 72	O II—19			1
4138 62	Fe II—39			1
4143 76	He I—53	7 s	8 s	
4151 63	Fe II—12			0
4153 18	O II—19			1
4156 50	C III—21, O II—19			1
4161 38	Fe II—39			0
4162 62	C III—21			1
4168 98	He I—52	1 N	2 N	
4173 57	Fe II—27	3 n	4 n	
4177 57	Fe II—21			1
4178 88	Fe II—28	3	4	
(4180 6)	[Fe V]	1 NN	2 NN	
4183 07	Fe II—21			0
4185 47	O II—36			1
4186 91	C III—18			1
4189 92	O II—36			2
4195 91	N III—6	3 NN	3 NN	
4199 98	N III—6	4 NN	4 NN	
4205 54	Fe II—22			1
4220 02	Ca II—16			0
4233 18	Fe II—27	3	5	
4244 42	[Fe II], Fe II—12	2	3	
4251 48	Fe II—12			0
4258 13	Fe II—21, Fe II—28	1	2	

TABLE 4—Continued

λ^*	IDENTIFICATION	INTENSITY		
		Pd 2166	Pd 2764	I'
4267 22	C II—6	3 N	4 N	
4273 30	Fe II—27	1 n	2 n	
(4276 9)	[Fe II]	0	0	
4278 10	Fe II—32	2	2	
(4287 5)	[Fe II]	1	1	
4296 52	Fe II—27	2 s	4 s	
4303 28	Fe II—27	1	2	
4314 36	Fe II—32			0
4319 52	O II—2, [Fe II]	2 N	5 N	
4330 61	N III—10			1
4338 60	He II—3, Fe II—32			0
4340 52	H γ	18	20	
4345 68	O II—2	1	2	
4348 28	N III—10			1
4349 30	O II—2	2 n	5 n	
4351 77	Fe II—27	2	4	
4359 49	[Fe II], O II—26	2	2	
4363 21	[O III]	12 NN	14 NN	
4367 04	O II—2	1 NN	3 NN	
4369 41	Fe II—28	1	2	
4371 91	Fe II—33			0
4378 74	N III—17	2 NN	3 NN	
4384 32	Mg II—10, Fe II—32	1	3	
4385 32	Fe II—27	1	3	
4386 33	Fe II—26			0
4387 89	He I—51	10 s	11 s	
4397 10	Fe II—33			0
4399 85	Fe II—20			1
4406 23	O II—26			0
4413 35	[Fe II], Fe II—32			1
4414 69	O II—5			0
4416 87	O II—5, Fe II—27, [Fe II]			2
4420 97	Fe II—9			1
4437 46	He I—50	2	5	
4447 99	O II—35, O III—33			1 NN
(4458 0)	[Fe II]	1	1	
4461 45	O III—33, Fe II—26			1
4465 36	N II—21			0
4471 69	He I—14	8 N	12 N	
4472 89	Fe II—37			1
4477 62	N II—21			0
4479 25	Ca II—6			0
4481 12	Mg II—4	2 Nd	2 Nd	
4488 14	N II—21			0
4489 17	Fe II—37	2 n	4 n	
4491 37	Fe II—37	3 n	5 n	
4508 29	Fe II—38	3 NN	4 NN	
4511 06	N III—3	4 n	5 n	
4515 29	Fe II—37, N III—3	5 N	5 N	
4520 24	Fe II—37	3	4	
4522 54	Fe II—38	1	1	
4523 56	N III—3			1
4525 84	Fe II—9			1
4534 42	N III—3, Fe II—37			1
4541 57	Fe II—38	4 NN	6 NN	
4549 46	Fe II—38	3	2	
4552 71	Si III—2			1
4555 98	Fe II—37	4	5	
4567 98.	Si III—2	...		2

TABLE 4—Continued

λ^*	IDENTIFICATION	INTENSITY		
		Pd 2166	Pd 2764	I'
4571 04	Mg I—1	5	5	
4576 38	Fe II—38	4 N	4 N	
4577 69	Fe II—54	1	2	
4580 14	Fe II—26			1
4582 73	Fe II—37	2	3	
4583 82	Fe II—38	5 N	4 N	
4590 85	O II—15	1	1	
4596 12	O II—15	2	2	
4601 38	N II—5, Fe II—43	..		1
4620 57	Fe II—38	2 n	3 n	
4629 36	Fe II—37	5 s	6 s	
4631 64	Si IV—6			1
4634 11	N III—2	8 N	8 N	
4638 75	O II—1	1	2 NN	
4640 64	N III—2	9 N	10 N	
4641 79	N III—2, O II—1	3 N	4 N	
4644 20	Fe II—31	..		1
4647 42	C III—1	8 N	9 N	
4649 20	O II—1, Fe II—25	4 N	5 N	
4650 27	C III—1, O II—1	5 N	6 N	
4651 25	C III—1, O II—1	2 N	3 N	
4661 48	O II—1			1
4663 92	Fe II—44		..	1
4666 65	Fe II—37	3	3
4676 42	O II—1			1
4685 77	He II—1	18	20	.. .
4713 37	He I—12	8 N	10 N	..
(4725) ..	[Ne IV]	6 NNN	8 NNN	
4731 78	Fe II—43	2 n	2 n	
4861 43	H β	22	25	
4921 96	He I—48	9 n	11 n	
4958 9†	[O III]	2 NN	3 NN	
5006 8†	[O III]	5 NN	9 NN	
5015 7†	He I—4	3 N	5	
5875 92	He I—11			12
6247 66	Fe II—74			1:
6300 41	[O I]			3
6347 16	Si II—2			2
6363 76	[O I]			1
6371 26	Si II—2			4
6416 45	Fe II—74:			4
6432 57	Fe II—40			5
6456 46	Fe II—74			4
6516 04	Fe II—40			6
6562 77	H α			50
6678 06	He I—46			16

number. The third and fourth columns give figures on the strength and quality of the stronger features, and some weak ones, estimated separately to provide a more consistent intensity scale for the IIa-O plates. The fourth column refers to the July, 1955, plate, and the fifth column to the 1956 plate. The fifth column gives a measure of the line strength, I' , for the weaker lines as estimated during measurement. Data for the one available red plate is also given in the fifth column, but the intensity scale has no overlap to relate it to the blue scale. Lines of strength 1 are fairly distinct but near the limit of certainty; 0 denotes very weak or imperfect lines. Some features have wave lengths in parentheses;

these were primarily some of the broad forbidden lines best interpolated on microphotometer tracings. Other lines, e.g., N1 and N2, were not measured and are listed with laboratory wave lengths marked by a dagger. Table 5 lists the measured wave lengths and possible identity of lines found on only one plate or where identity is otherwise doubtful. Many more lines like these remain unidentified, and many are probably spurious. All were given strength 0 or 1. Table 6 summarizes the number of lines and identifications in Tables 4 and 5 according to element and ionization stage. Absorption lines are not included in the tables, since the absorption spectrum is not well marked. A few strong lines of Fe I and Sr II were the only ones measured. The λ 4227 line of Ca I is present as a very broad feature and has already been discussed.

TABLE 5
WEAK EMISSION LINES DOUBTFULLY PRESENT IN MWC 603

λ	Identification	λ	Identification	λ	Identification
3609 71	C III—10	4085 01	O II—10	4460 07	N II—21
3632 38	Fe II—112	4087 44	Fe II—28	4474 96	O III—37
3634 30	He I—28	4109 88	Ca II—17	4507 72	N II—21
3713 18	Ne II—5	4110 79	O II—20	4529 40	O III—32
3725 20	O III—14	4113 76	O II—37	4555 01	O III—34
3727.47	O II—3	4120 06	O II—20	4558 68	Fe II—20
3732 86	He I—24	4158 29	Fe II—12	4602 74	Fe II—19
3737 19	Ca II—3	4160 68	Fe II—39	4606 87	N II—5
3825 07	Fe II—29	4215 40	N III—6	4621 46	N II—5
3832 40	Mg I—3	4227 22	Fe II—45	4627 51	Fe II—54
3838 25	Mg I—3	4227 65	N II—33	4630 56	N II—5
3867 65	He I—20	4239 67	O III—1	4634 75	Fe II—25
3882 75	O II—11,	4325 45	C III—7	4642 98	N II—5
	O II—12	4327 15	Fe II—20	4648 35	Fe II—38
3908 23	Fe II—29,	4347 42	O II—16	4657 12	Fe II—43
	O II—11	4357 07	O II—18	4669 86	Fe II—25
3911 66	O II—17	4375 09	N II—16	4673 57	O II—1
3954 04	O II—6	4380 94	Fe II—9	4705 74	O II—25
3955 59	N II—6	4395 69	O II—26	4709 83	O II—24
3981 76	Fe II—3	4428 25	Mg II—9	4718 34	Ca II—7
3985 37	O II—22	4434 21	Mg II—9	4720 28	Fe II—54
3995 47	N II—12	4439 14	Fe II—32	4722 48	Ca II—7
4001 69	Fe II—29	4440 08	O III—33	4724 00	Fe II—17
4007 83	He I—56	4447 10	N II—15	6368 94	Fe II—40
4041 73	Fe II—13	4452 16	O II—5,	6582 53	C II—2
			[Fe II]		

DISCUSSION

The two best spectrograms are the ones of July 12, 1955, and August 15, 1956, which reach from slightly below the Balmer limit to the N1 and N2 lines of [O III]. Longward of λ 3900 the two spectra are generally similar; shortward of λ 3900 they differ significantly. On the 1955 plate, hydrogen lines to H27 could be separated, and a weak Balmer continuum may be present. The general ultraviolet continuum is easily seen well beyond the Balmer limit. The large number of distinct Balmer lines at this date indicates a very low electron pressure in the region of hydrogen-line formation. The nearly uniform velocity of material over a wide range of time and the excitation and ionization stages suggest a relatively stable or stationary envelope; the observed velocity probably belongs to the star as a whole as well as to ejected material. The star is not entirely constant, however, since on the 1956 plate the ultraviolet continuum is nearly invisible and the hydrogen lines could be seen only to H19, although this plate is the best exposed of all. This indicates a considerable rise in electron pressure prior to the epoch of the 1956 plate.

The rise in pressure is further confirmed by the behavior of He I. In July, 1955, the He I singlets dominated the triplets, probably because of low-density fluorescent excitation. In August, 1956, the triplets were markedly strengthened. The implication is that increased electron density favored recapture radiation in the triplets. In July, 1955, the ratio $\lambda 4387/\lambda 4026$ was about 2, while in August, 1956, the ratio was about unity. The August, 1954, plates have a ratio greater than unity but not so large as 2, while the November, 1954, plate, although underexposed, shows the $\lambda 4026$ line very weakly, while $\lambda 4388$ is strong. The $\lambda 4026$ line in August, 1956, and certainly in November, 1954, was no stronger than the singlet line $\lambda 4009$. There is no significant change in excitation of the forbidden lines between the dates of the two best plates, but it is clear that pressure changes are present in strata where H and He I lines are formed.

The importance of the fluorescence excitation is interesting in view of the rather high-excitation level shown by MWC 603. For example, [Fe v] is well marked, and [Fe vi] is

TABLE 6*
SUMMARY OF LINES AND ELEMENTS PRESENT

ELEMENT	SOURCE AND NO OF LINES				DEFINITE		POSSIBLE	
	Table 4		Table 5		Per- mitted	For- bidden	Per- mitted	For- bidden
	Good	Blends	Good	Blends				
H	23	2			H			
He I	18	5	4		He I			..
He II	1	2			He II			
C II	1		1				C II:	
C III	5	6	2		C III			
N II	3	1	11				N II	
N III	10	6	1		N III			
O II	21	16	14	4	O II			O I
O III	9	5	6		O III	O III		
Ne II			1			Ne III		Ne IV
Mg I	1		2		Mg I			
Mg II	1	2	2		Mg II			
Si I		2			Si I			
Si II	4				Si II			
Si III	2						Si III	
Si IV	3				Si IV			
Ca II	4	1	4		Ca II			
Ca III	1						Ca III	
Fe II	59	16	22	1	Fe II	Fe II Fe V		Fe VI
[O I]	2							
[O III]	3							
[Ne III]	2							
[Ne IV]		1						
[Fe II]	4	7		1				
[Fe V]	2	7						
[Fe VI]	2	1						

* The forbidden lines include [Fe II], where the strongest features identified by Merrill (1928) in η Carinae are all weak but present. These features tend to be sharp compared to the other forbidden features. [S II] almost certainly contributes to abnormally strong lines of C III and O II, with which it is blended. One line of [Fe V] further complicates the region near the $\lambda 4068, \lambda 4076$ pair of [S II] lines, but there seems little doubt that they contribute some of the intensity. The red [S II] lines are not seen. At about $\lambda 4725$ a moderately strong and rather broad emission feature is seen. No known permitted radiation seems to account for $\lambda 4725$, and from its fuzzy character it suggests forbidden radiation. A group of four [Ne IV] lines are given in the *Revised Multiplet Table* between $\lambda 4715$ and $\lambda 4721$ with considerable uncertainty as to the precise wave length. From the strength of [Ne III] and the presence of high excitation, indicated by [Fe V] and [Fe VI], the presence of [Ne IV] would not be surprising. In the red region two lines matching with [O I] are present; the identification is not certain, although no other known lines have these wave lengths. $\lambda 3727$ of [O II] is not present. The most definite forbidden lines are discussed in the text.

virtually certain, although weak. In RW Hydrae the $\lambda 4388/\lambda 4026$ He I ratio is about 2 (Swings and Struve 1942), but the excitation level is lower than in MWC 603. When at low stages of excitation, CI Cygni and AX Persei resemble MWC 603, but the helium triplets still dominate or remain nearly as strong as the singlets. The presence of the recombination spectra of O III and N III links MWC 603 with the lower-excitation object RW Hydrae, but the nebular resonance excitation mechanism by He II $\lambda 303$ suggested by Bowen (1935) is operative in MWC 603 and not in RW Hydrae. The only O III line in our spectral region affected by the Bowen mechanism is $\lambda 3759$, which is clearly enhanced, as are the expected N III lines. Also unlike RW Hydrae, C III apparently is present in MWC 603. It appears that an important feature in MWC 603 is that stratification in the place of origin causes the excitation to vary from element to element.

To illustrate this problem further, the variation in line sharpness must be considered. The triplets of He I vary in sharpness with respect to the singlets accompanying the variation in singlet/triplet ratios. The singlets are sharp, notably the $\lambda 3965$ line of the $2^1S-4^1P^0$ transition and the lines of the $2^1P^0-n^1D$ transition. The leading lines of the $2^1P^0-n^1S$ transition are weakly present and are, on the whole, less sharp, although this is partially an intensity effect. The Mg I and Si I lines and lines of the lowest multiplet of Si II are quite sharp; Si III may be present but is very weak, while the leading lines of Si IV appear to be present but are weak and quite diffuse. Fe II lines are, on the whole, sharp; strong, low-level lines at $\lambda 3938$ and $\lambda 3914$ are perhaps the sharpest features in the spectrum. They arise from the a^4P level at 1.6 volts. Higher lines arising from the b^4P and b^4F levels at 2.8 volts are distinctly less sharp and sometimes markedly soft. Lines of O II are slightly diffuse, but O III, N III, and C III give broad or very broad lines. The higher members of the Balmer series and H and K are somewhat soft. He II $\lambda 4686$, exceeded in strength only by $H\alpha$ and $H\beta$, is quite sharp. $H\alpha$ completely dominates the red spectrum and may have a strength greater than the sum of all other emission lines. The hydrogen lines show incipient structure. The fuzziest features, omitting blends, are the forbidden lines. [O III] is represented by $\lambda 4363$ and N1, with N2 apparently present but weak. [Ne III] is represented by the pair of lines in the ultraviolet. Particularly interesting are the [Fe V] lines. All the lines given by Swings and Struve (1942) for AX Persei in early 1942 are present in our spectral region except $\lambda 4003$, which is not certain in AX Persei. The intensities are somewhat reduced in MWC 603, but the pattern is the same. The lines are all extremely diffuse. [Fe VI] is possibly present, based upon the two lines strongest in AX Persei. A model for MWC 603 must fit the picture presented by the line widths. They seem to be correlated with excitation and ionization in the case of Fe, Si, and the C, N, O group. He I is sharp, indicating formation in a zone of small internal streaming or turbulent motions, while the forbidden lines of high ionization such as [Fe V] are very broad, suggesting very turbulent motion. Some lines such as Si I and Ca II may belong to the late-type source rather than to the nebula. Some of the permitted C, N, O features might be explained by the presence of a very hot star, but nebular conditions clearly dominate, as evidenced by the Bowen mechanism in C III and N III and fluorescence in He I. Over the time covered by our observations, however, the configuration has been stable, with nearly constant velocity independent of place of origin of the lines. The sharpest lines have a width, at half-intensity, of about 50 km/sec, while the resolution corresponds to about 40 km/sec. The H and He I lines average about 60 km/sec (higher-series members), [Ne III] is about 100 km/sec wide, while very diffuse lines like [O III] and [Fe V] average 150 km/sec. Thus the macroscopic stability, in the presence of such large motions, becomes even more surprising.

The over-all spectral characteristics of MWC 603 are intermediate between the high-excitation symbiotic systems like AX Persei and CI Cygni and the lower-excitation object RW Hydrae. The light-variation during our period of observation has been small and was appreciable only in the ultraviolet; it has some resemblance to that in old novae or in T Coronae Borealis at minimum. Independent variation of red and blue sources occurs

in many, if not all, symbiotic systems. The high space velocity and the apparent stability of MWC 603 are its distinguishing features. MWC 603 seems likely to prove an interesting addition to a group of slow, nova-like peculiar emission objects. These may have considerable significance in stellar evolution, possibly representing a fairly rapid stage of evolution, with rapid loss of mass such as discussed by Deutsch (1956*a*, *b*) for single stars, or in binaries.

REFERENCES

- Bowen I. S. 1935, *Ap. J.*, **81**, 1
Deutsch, A. J. 1956*a*, *Pub. A.S.P.*, **68**, 308.
———. 1956*b*, *Ap. J.*, **123**, 210.
Greenstein, J. L., MacRae, D. A., and Fleischer, R. 1956, *Pub. A.S.P.*, **68**, 242
Hulst, H. C. van de, Muller, C. A., and Oort, J. 1954, *B.A.N.*, Vol **12**, No 452
Johnson, H. L., and Morgan, W. W. 1953, *Ap. J.*, **117**, 313.
Merrill, P. W. 1928, *Ap. J.*, **67**, 391.
Merrill, P. W., and Burwell, C. G. 1943, *Ap. J.*, **98**, 153.
Swings, P., and Struve, O. 1942, *Ap. J.*, **96**, 254.
Walker, M. G. 1954, *Pub. A.S.P.*, **66**, 71.